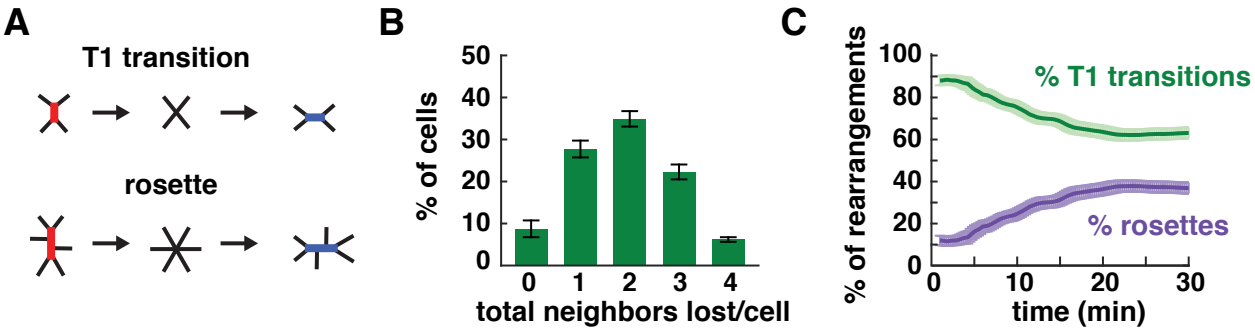

Fig. S1. Contributions of T1 transitions and rosette rearrangements to *Drosophila* axis elongation. (A) Schematics of a T1 transition (top) and rosette formation and resolution (bottom). (B) Percentage of cells that lost the indicated number of neighbors by t = 30 min. (C) Percentage of cell rearrangements that occurred through T1 transitions (green) or rosettes (purple). A single mean value was obtained for each embryo and the mean±sem between embryos is shown (n = 7 wild-type (WT) Spider:GFP embryos, average of 240 cells tracked for at least 50 time points in each movie, images acquired every 15 s).

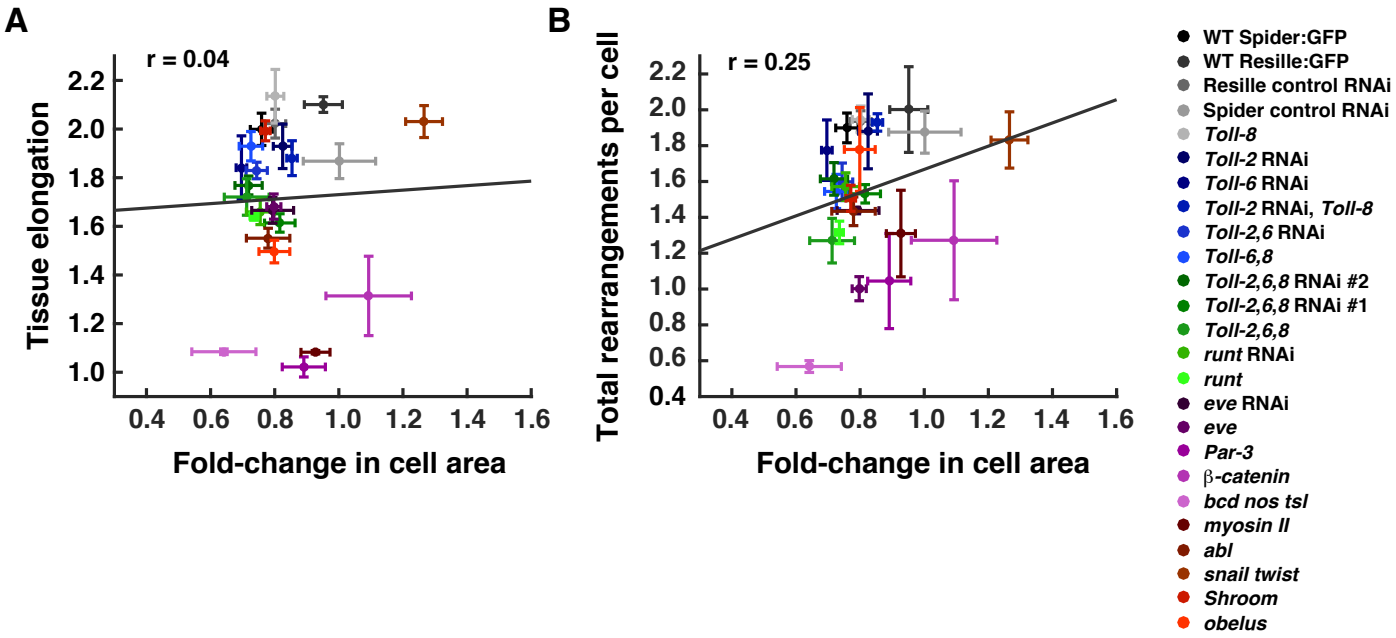

Fig. S2. Relationship between apical cell area, cell rearrangement, and tissue elongation across genotypes. (A,B) Fold-change in apical cell area (between t = 0 and t = 30 min) vs. tissue elongation (A) or total cell rearrangements (B). A single mean value was obtained for each embryo and the mean±sem between embryos is shown (n = 3-8 embryos/genotype except myosin II, n = 2). R, Pearson's correlation coefficient.

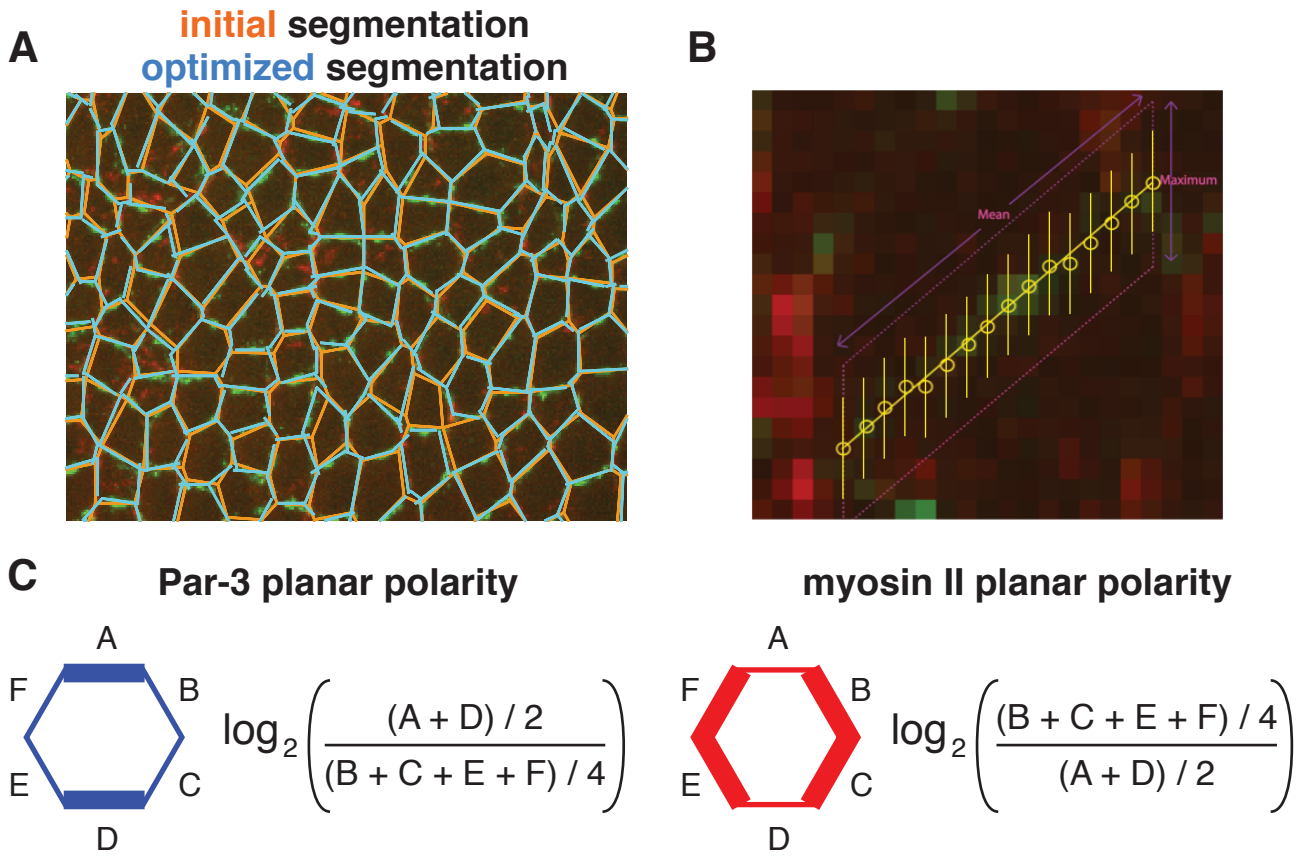

Fig. S3. Tools to analyze cortical planar polarity in SEGGA. (A) Vertex positions in the segmentation were automatically shifted locally to optimize the overlap with the maximum intensity pixels in the image. (B) Edge intensity was the average of the maximum intensities along 5-pixel lines intersecting the edge. (C) Par-3 planar polarity was the $\log_2$ ratio of the average intensity at transverse edges (0-30°) relative to vertical edges (60-90°) and myosin II, F-actin, and Shroom planar polarity were the $\log_2$ ratios of the average intensity at vertical edges relative to the average intensity at transverse edges (0° is parallel to the AP axis).

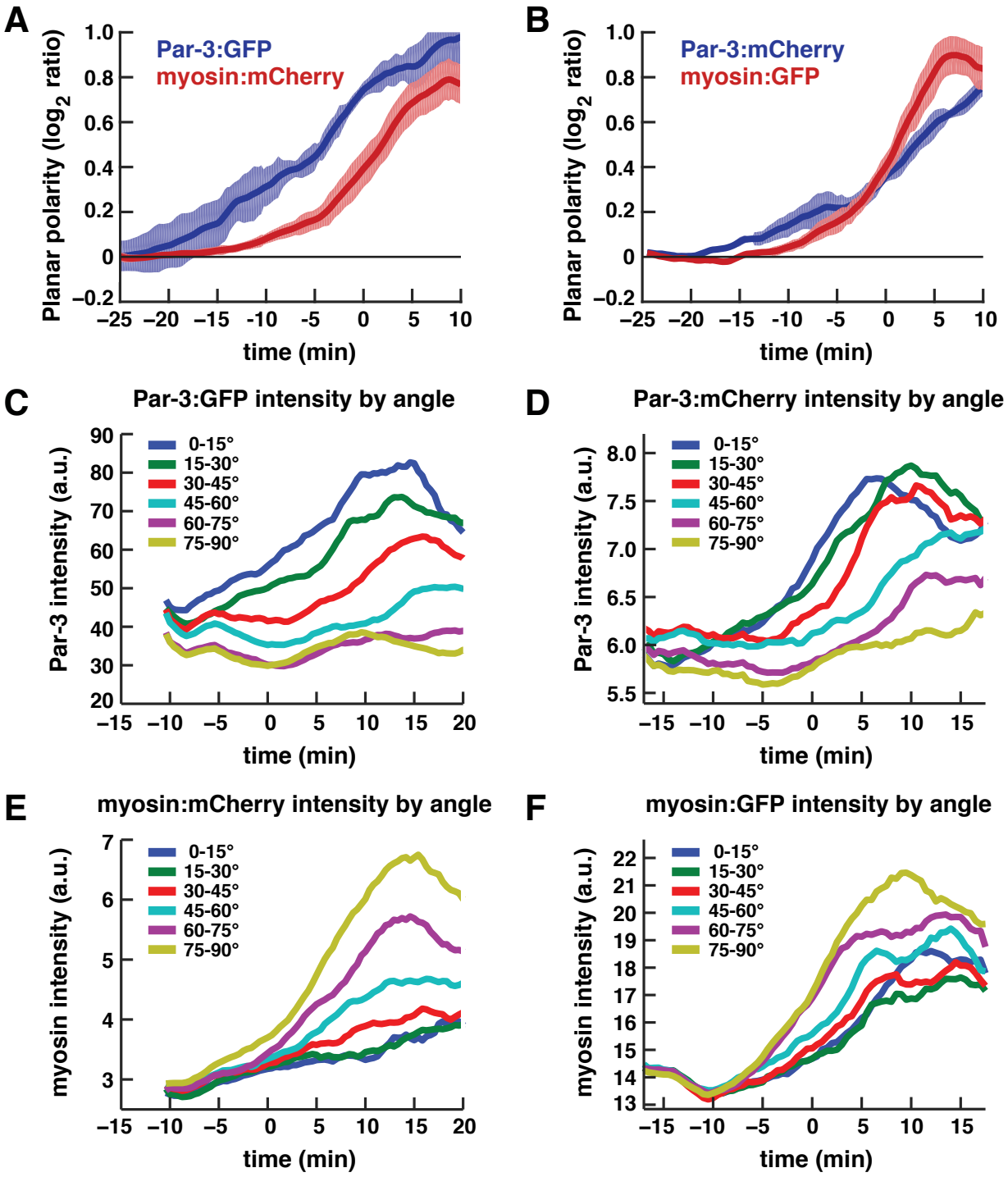

Fig. S4. Par-3 and myosin II planar polarity analysis with the fluorophores reversed. (A,B) Plots show the $\log_2$ ratio of Par-3 at transverse (0-30°) to vertical (60-90°) edges or the $\log_2$ ratio of myosin II at vertical to transverse edges in embryos coexpressing both markers tagged with different fluorophores (0° is parallel to the AP axis). A single mean value was obtained for each embryo at each time point and the mean±sem between embryos is shown (n = 4 movies/condition, an average of 290 cells/time point were analyzed for each movie). Par-3 planar polarity preceded myosin II planar polarity in both cases. (C-F) Average edge intensities binned by angle in a single Par-3:GFP; myosin:mCherry movie (average of 1097 edges analyzed/time point) (C,E), and a single Par-3:mCherry; myosin:GFP movie (average of 823 edges analyzed/time point) (D,F).

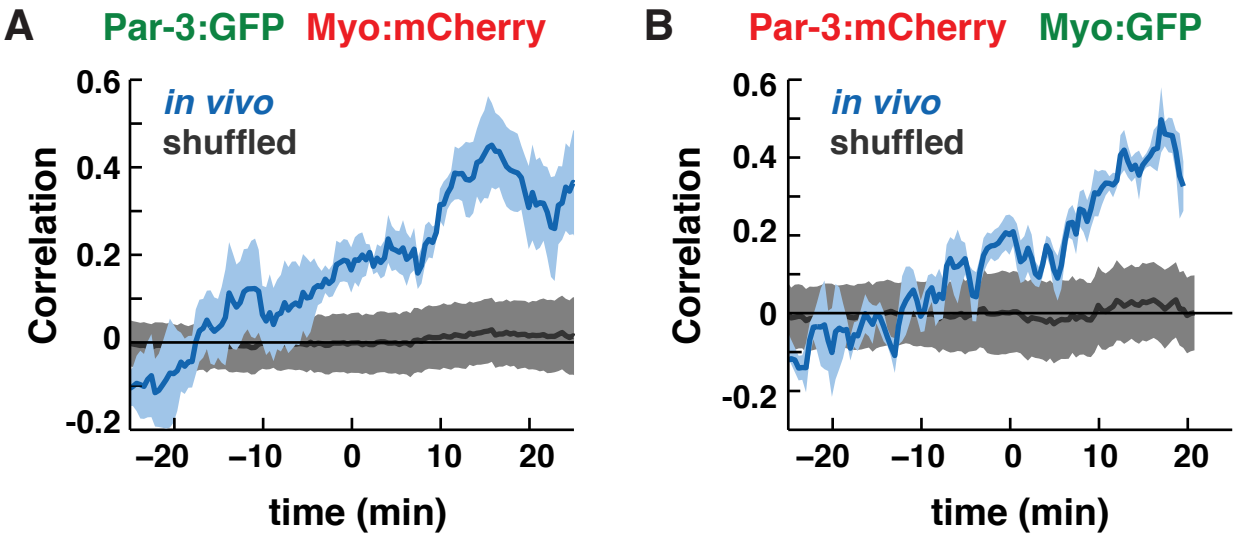

Fig. S5. Par-3 and myosin II planar polarities are spatially correlated.
(A,B) Cell-by-cell correlation of Par-3 and myosin II polarity (mean±SD). Blue curves, correlations between the extent of Par-3 and myosin II planar polarity. Black curves, correlations recalculated after edge values were shuffled within 5° bins (n = 4 movies/condition, an average of 290 cells/time point were analyzed for each movie).

Supplementary Materials and Methods

Fly stocks and genetics. In this study we expanded on our previous analysis in SEGGA of the published movies described in this section (movies not previously published are described in the main paper). The following published wild-type movies were further analyzed in this study: Spider:GFP and Resille:GFP (Paré et al., 2014), Spider control RNAi (Spider:GFP embryos injected with *flp* dsRNA) (Simões et al., 2014), Resille control RNAi (Resille:GFP embryos injected with *Toll-3* dsRNA) (Paré et al., 2014), and two-color movies of Par-3 and myosin II generated by Sérgio Simões (Simões et al., 2010) using sqh-sqh:mCherry (the myosin II regulatory light chain fused to mCherry) (Martin et al., 2009) and UAS-Baz:GFP (Par-3 fused to GFP) (Benton and St Johnson, 2003).

The following published mutant movies were further analyzed in this study: *abl*^{4} maternal mutants (the progeny of females bearing *abl*^{4} germline clones) expressing arm-arm:GFP (β-catenin) (Tamada et al., 2012), *eve*^{R13} and *runt*^{LB5} zygotic mutants expressing Spider:GFP (Paré et al., 2014), *eve* RNAi (Spider:GFP embryos injected with *eve* dsRNA) (Paré et al., 2014), *runt* RNAi (Spider:GFP embryos injected with *runt* dsRNA) (Paré et al., 2014), *obe*^{1} maternal mutants (the progeny of homozygous *obe*^{1} females) expressing Resille:GFP (Vichas et al., 2015), *Shroom* null mutants (the progeny of *Shroom*$^{\Delta 11}$/Df(2R)Exel7131 females and males) expressing Spider:GFP (Simões et al., 2014), *bcd nos tsl* maternal mutants (the progeny of *bcd*^{E1} *nos*^{L7} *tsl*^{146} homozygous females) expressing Resille:GFP (Blankenship et al., 2006), and myosin II (*sqh*^{1}) maternal mutants (the progeny of females bearing *sqh*^{1} germline clones) expressing Spider:GFP (Simões et al., 2010). *Par-3* maternal and maternal/zygotic mutants (the progeny of females bearing *baz*^{GD21} germline clones) (Simões et al., 2010) were combined in Figure 3E-H, and only the more severe Par-3 mutant embryos (likely maternal/zygotic mutants) were used for the analysis in Figure 4 and Figure S2. *Toll-2,6,8* single, double, triple mutants were generated as described (Paré et al., 2014) as zygotic mutants or embryos injected with dsRNA. These genotypes were: *Toll-2* RNAi (Resille:GFP + *Toll-2* dsRNA); *Toll-6* RNAi (Resille:GFP + *Toll-6* dsRNA); *Toll-8* (Resille:GFP; *Toll-8*$^{59/145}$); *Toll-2,6* RNAi (Resille:GFP + *Toll-2* and *Toll-6* dsRNAs); *Toll-2* RNAi, *Toll-8* (Resille:GFP; *Toll-8*$^{59/145}$ + *Toll-2* dsRNA); *Toll-6,8* (*Toll-2*$^{\Delta 76}$/CyO; *Toll-8*^{59}, *Toll-6*^{5A}, Spider:GFP); *Toll-2,6,8* RNAi #1 and #2 (Resille:GFP; *Toll-8*$^{59/145}$ + two independent sets of *Toll-2* and *Toll-6* dsRNAs as described in Paré et al., 2014); and *Toll-2,6,8* (*Toll-2*$^{\Delta 76}$; *Toll-8*^{59}, *Toll-6*^{5A}, Spider:GFP) (Paré et al., 2014).

Image processing. Several methods can be applied empirically by the user in SEGGA to reduce noise in the images, including multiplying pixel intensities in three consecutive apical z-planes and normalizing the intensities to occupy the full intensity range, background subtraction, contrast enhancement, erosion and dilation, smoothing with a Gaussian filter, and other custom image processing algorithms. Image processing techniques involve a combination of built-in functions in the MATLAB Image Processing Toolbox and custom image processing algorithms. Some open-source, third-party algorithms and applications for image processing and analysis were incorporated into SEGGA. These are noted in the code where applicable, and some are described in previous publications (Perona and Malik, 1990; Gerig et al., 1992; Lienkamp et al., 2012; Theilicke and Stamhuis, 2014).

Image segmentation. Segmentation functions in SEGGA apply two different algorithms to a region of interest defined by the user. In the first method, a series of thresholding functions in MATLAB are applied to the image, in addition to any image processing steps specified by the user. The image is then thresholded and skeletonized to produce the initial segmentation. In the second method, we implemented a novel segmentation algorithm that expands concentric circles initiated at all non-boundary pixels. This technique starts at low-intensity regions and exploits the convex and relatively isotropic geometries of epithelial cells. Briefly, a single circle is assigned to each cell in the thresholded image based on five criteria. (1) For each zero-value pixel, if no boundary pixels exists in an area of a minimum radius, then a circle exists for that pixel. (2) The radius of the circle is increased until this criterion no longer holds. (3) This function is applied to all pixels. (4) Duplicate circles are eliminated by keeping only the largest of each set of overlapping circles. (5) For adjacent circles that have no boundary pixels between them, the smaller circle is removed.

The skeletonized threshold generated by the first method is then modified using information from the placement of circles in the second method to improve the accuracy of segmentation. Cells below a minimum size are automatically corrected by merging small cells with a neighboring cell by removing one edge. The edge that is removed is chosen in order to minimize the change in angles of the remaining edges. The result is a skeletonized image of 1 pixel-wide cell boundaries that is used to determine the placement of nodes and edges in the segmentation. Groups of nodes associated with individual cells are sequentially connected based on angle with respect to the cell center, resulting in a continuous lattice of convex polygons.

Error correction. Semi-automated error corrections can be made within the region of interest to improve the accuracy of segmentation. To analyze cell behavior, 100% of cells need to be correctly tracked. This is achieved through a user-guided, semi-automated correction process. A subset of time points at regular intervals (in this study, every 20th time point, or every 5 min in real time) are manually corrected by the user. Errors in tracking are displayed in a graphical user interface that provides a range of annotation capabilities. Users can alter cell geometry by moving nodes, alter cell topology by collapsing an edge to a node or expanding a node to an edge, and alter cell number by adding an edge to divide one cell into two or by removing an edge to merge two cells into one. Additional tools are provided to correct less common errors.

To achieve isomorphic mapping to the reference frame, the time points immediately before and after each reference frame also need to be corrected. Manually corrected images are then used as reference frames for the automated propagation of corrections to other time points in the image sequence. Automatic propagation compares every pair of consecutive time points and adds or removes edges if a cell is missing in one of them. The decision to add an edge to the frame with a missing cell or remove an edge from a frame with an extra cell is made with preference to the frame closer to the corrected frame. For edges that are added, the new node positions take into account node positions at the adjacent frame and the lattice movement between the two frames. This semi-automated framework can be repeated as needed until 100% accurate tracking is achieved.

Cell tracking. Cells were tracked using a nearest neighbor search, and the tracks of successfully tracked cells were used to improve the tracking of other cells. Untracked cells were shifted by the average displacement of correctly tracked cells at that time point. In addition, the average displacement of correctly tracked cells at one time point was used to improve the tracking at the next time point. In these cases, for two consecutive time points, A and B, untracked cells in B are shifted by the average local displacement of correctly tracked cells between A and B before performing a nearest neighbor search at the next time point. These steps are repeated until all cells in the region were successfully tracked or after five iterations, whichever comes first. Any remaining untracked cells are flagged as errors in the user interface. Dividing, delaminating, and inserting cells are flagged as errors and can be categorized by the user as a cell division, delamination, or insertion event using the “classify error” button in the user interface. For dividing cells, the mother cell is manually associated with two daughter cells in the first post-division time point through the user interface.

Temporal registration and selection of cells for analysis. Movies of different embryos were temporally registered based on the time of onset of tissue elongation, which corresponds to the beginning of stage 7. Tissue length shows a clear minimum at the onset of cell intercalation and displays a monotonically increasing trend that provides a readily identifiable developmental timescale across embryos. The SEGGA Single Movie Analysis window provides a plot of tissue length over time that allows the user to manually set the t = 0 time point. As all movies focused on the anterior and central regions of the ventrolateral germband epithelium, registration in space was not performed.

Movies were segmented until the first cell divisions occurred within the anterior ventrolateral germband, at the end of the fast phase of germband extension in late stage 8, which is approximately 30 min after the onset of elongation. As all germband extension movies ended at the same, objectively defined reference point defined by the onset of cell division, for any given measurement the last value of the movie was extended until t = 30 min (or the last time point at which any movie was analyzed, whichever came first) and was used as the end condition for statistical analysis for movies that ended slightly before t = 30 min.

Different criteria were used to select groups of cells analyzed for different measurements, which can be modified by the user in the Single Movie Analysis window. For static measurements that do not require tracking, all cells in the corrected region were analyzed. For tissue elongation, a contiguous group of cells that were in the corrected region at all time points was used. Measurements that require cell or edge tracking can be restricted to cells that are within the corrected region for a minimum number of time points defined by the user. In this study, for measurements that require tracking, cells were included in the analysis if they were in the corrected region for at least 50 time points (12.5 min) after the onset of elongation (t = 0). This value was chosen empirically to maximize the number of cells that could be analyzed long enough to capture cell rearrangement. An edge was scored as shrinking if it started off at least 12 pixels in length, was tracked for at least 20 time points (5 min), and remained fully contracted for at least 5 time points.

Static measurements (cell scale)

Cell area. The area of the region bounded by the perimeter of each cell.

Cell area coefficient of variation. The standard deviation of the cell area distribution divided by the mean of this distribution.

Cell eccentricity. The square root of 1 minus the squared ratio of the span of the short axis to the span of the long axis of an ellipse fit to each cell. An isotropic, circular cell yields a value of zero and a highly anisotropic cell yields a value approaching 1.

Cell horizontal length. The horizontal span of an ellipse fit to each cell, using the eigenvalues of the inertia tensor to determine the major and minor axes of the ellipse.

Cell horizontal-to-vertical length ratio. The ratio of the widest horizontal span to the widest vertical span of an ellipse fit to each cell.

Cell orientation. The angle of the long axis of an ellipse fit to each cell, relative to the horizontal axis of the image, calculated on a scale of 0-180°.

Cell rectangularity. The average of the normalized difference between each internal angle and the nearest factor of 90 degrees. This value is normalized to 45, the furthest angular distance from any multiple of 90.

Cell vertical length. The vertical span of an ellipse fit to each cell, using the eigenvalues of the inertia tensor to determine the major and minor axes of the ellipse.

Cell vertical to horizontal length ratio. The ratio of the widest vertical span to the widest horizontal span of an ellipse fit to each cell.

Node multiplicity. The average number of edges meeting at each vertex (node).

Normalized measurements. The following measurements are also provided as measurements normalized to the value at the t = 0 time point selected by the user: cell area, cell horizontal length, cell vertical length, and cell horizontal to vertical length ratio.

Number of neighbors. The average number of edges of a cell.

Pattern deformation (Texture tensor). The variance of the distance between the geometric center of each cell and the geometric centers of its neighbors, as defined in equation 6 of Graner et al., 2008 (Graner et al., 2008; Guirao et al., 2015).

Topological disorder. The variance of the number-of-sides distribution (as described in Zallen and Zallen, 2004).

Vertical edge alignment. The percentage of edges oriented at 75-90° relative to the horizontal axis that were connected to at least one other edge oriented at 75-90° relative to the horizontal axis.

Static and dynamic measurements (tissue scale)
Tissue dimensions are calculated using the eigenvalues of the inertia tensor taken from the cell centers for a group of cells. All tissue measurements are applied to a contiguous group of cells selected by the user and are calculated during the period that the entire group is tracked. All elongation measurements are normalized to the value at the user-selected t = 0 time point, except for tissue aspect ratios, which are provided either as ratios or as normalized ratios. Tissue-scale measurements include tissue horizontal elongation, vertical elongation, long axis elongation, short axis elongation, tissue horizontal-to-vertical aspect ratio, tissue long axis to short axis aspect ratio, normalized tissue horizontal-to-vertical aspect ratio, and normalized tissue long axis to short axis aspect ratio.

Dynamic measurements (cell scale)
Only cells tracked for at least 50 time points (12.5 min) after t = 0 were included in this analysis.

Neighbors lost per cell. The number of edges that disappeared and did not reappear for 10 or more frames (2.5 min) divided by the total number of tracked cells. The contracting edge must be at least 6 pixels (2 μm) long at some point before contracting. These events do not require the formation of a new edge that separates the pair of cells that were initially connected. The time point assigned to a neighbors lost event is the mean time point between the first frame when the shrinking edge disappeared and the last frame after which the shrinking edge no longer reappeared. The time point assigned to a rosette event is the mean of all individual edge contraction events contributing to the rosette.

T1 transitions per cell. The number of edges that contracted into a 4-cell vertex and did not reform or join a higher-order vertex before resolving, divided by the total number of tracked cells.

Rosettes per cell. The number of edges that contracted into a vertex and did not reform or resolve before joining a higher-order vertex containing 5 or more edges, divided by the total number of tracked cells.

Neighbors gained per cell. The number of edges that formed from a vertex of 4 or more cells and did not contract back to a vertex during the course of the movie, divided by the total number of tracked cells.

Histogram of neighbors lost. The percentage of cells that lost 0, 1, 2, 3, or ≥4 edges that contracted to join 4-cell vertices (T1 transitions) or higher-order vertices containing 5 or more edges (rosettes).

Histogram of T1 transitions. The percentage of cells that lost 0, 1, 2, 3, or ≥4 edges that contracted to join 4-cell vertices.

Histogram of rosettes. The percentage of cells that lost 0, 1, 2, 3, or ≥4 edges that contracted to join higher-order vertices containing 5 or more edges.

Histogram of neighbors gained. The percentage of cells that gained 0, 1, 2, 3, or ≥4 edges.

Dynamic measurements (nodes and edges)
Rate of edge contraction. The average rate of change in edge length over a 15-frame window, calculated only for edges that contribute to a neighbors lost event (see previous section).

Rate of edge growth. Same criteria as above for all edges that appear during the course of the movie with the time axis reversed.

Node resolution. Node resolution times are analyzed for all nodes at which 4 or more cells meet. Measurements are provided in minutes for all nodes (all resolution times), nodes at which 4 cells meet (T1 resolution times), and nodes at which 5 or more cells meet (rosette resolution times). Resolution time is measured as the difference between the time an edge contracted to a vertex and the first time point at which the two cells initially in contact were no longer in contact through a shared edge or vertex, provided that they do not reestablish contact for at least 10 time points (2.5 min). All cells contacting the vertex must be in the corrected region for at least 40 time points (10 min) after vertex formation to exclude vertices that quickly leave the field of view.

Planar polarity analysis. Planar polarity for myosin II, Shroom, and F-actin was calculated for each cell as the $\log_2$ ratio of the fluorescence intensity at vertical edges (oriented at 60-90° relative to the anterior-posterior axis) to the intensity at transverse edges (oriented at 0-30° relative to the anterior-posterior axis). Par-3 planar polarity was the $\log_2$ ratio of the intensity at transverse to vertical edges. Cells without at least one edge in each category were excluded from the analysis. This method does not distinguish between bipolar and unipolar cells, which can be distinguished by other methods (Tetley et al., 2016).

The intensity value assigned to an edge is the mean of all pixel intensity values along the edge. Each pixel intensity value was measured by taking the maximum intensity along a 5-pixel horizontal or vertical line centered at that pixel. Search lines are adjacent, nonoverlapping, and leave no gaps. To improve the overlap between the segmentation and the cell boundaries, edge placement was optimized to maximize overlap with the highest total pixel intensity values in the underlying image. First, edge position was averaged over three consecutive time points and the results were then smoothed over three time points using the average values. Second, for each edge, both nodes were shifted by up to 3 pixels (1 μm) along the x and y axes, allowing edges to rotate, translocate, and increase or decrease in length within a limited region. Edges that share a node were moved independently, and the position that maximized the overlap with the underlying signal was the highest weighted average of the intensity of all edges that meet at that

node, with each edge weighted by length and the edge under analysis given double weighting. Edge position was maximized independently for each edge. Local noise correction was used to control for variations in fluorescence intensity and tissue curvature across the image by calculating the mean intensity from the centers of the 20 nearest cells and subtracting the 25th percentile value.

Annotations and color maps. Preset color maps showing various measurements superimposed on the image data are available for cell area, cell eccentricity, cell horizontal-to-vertical length ratio, cell polarity, cell rearrangements, cell topology, pattern deformation, and rosette behaviors, among other measurements. In addition, various classes of edges can be highlighted, including all shrinking edges, shrinking edges that lead to T1 transitions, shrinking edges that lead to rosette formation, and growing edges (newly formed edges that occur as the result of vertex resolution). A bipolar color map highlights the mean instantaneous edge velocity of shrinking and growing edges.

Default bounds of the color maps are provided in SEGGA and these bounds can be modified by the user. Users can generate custom color maps using any number of colors and value ranges for discrete color maps, as well as linear and nonlinear color gradients interpolated through any number of colors for continuous color maps. Color maps can be applied to additional measurements with minimal code development. Users can create and compare custom color maps, apply them to any image analyzed in SEGGA, and edit and save these maps in real time without a requirement for hard coding modifications.

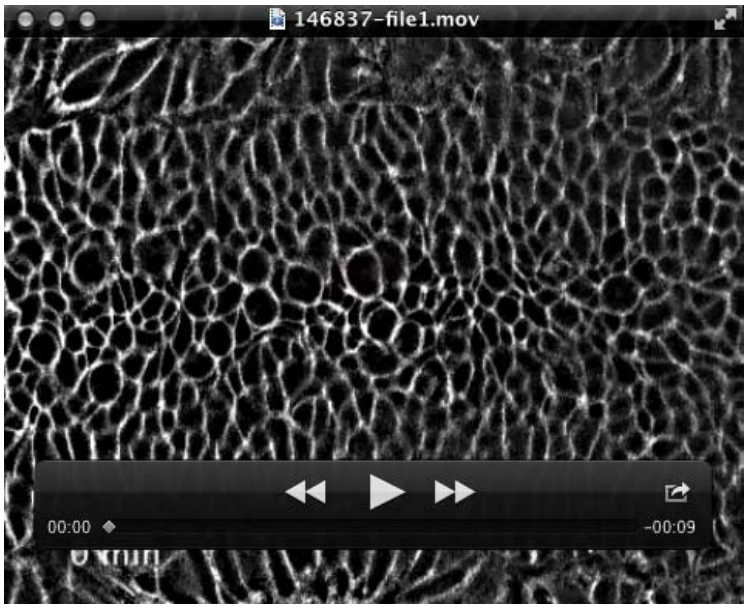

Movie 1. Cell division in the mouse spinal neural plate. Wild-type embryo expressing a membrane-localized GFP produced by epiblast-specific recombination of an mT/mG reporter using Sox2-Cre (Muzamdar et al., 2007; Williams et al., 2014). Time indicated in min starting at E8.0, images acquired every 6 min. Anterior left, ventral view.

Movie 2. Cell rearrangements during *Drosophila* axis elongation. Wild-type embryo expressing Spider:GFP. Time indicated in min:s, images acquired every 15 s. Anterior left, ventral down. Cells that lost neighbors were highlighted starting at t = 0 (the onset of elongation in stage 7). Purple, no neighbors lost. Blue, one neighbor lost. Green, two neighbors lost. Yellow, three neighbors lost. Red, four neighbors lost.

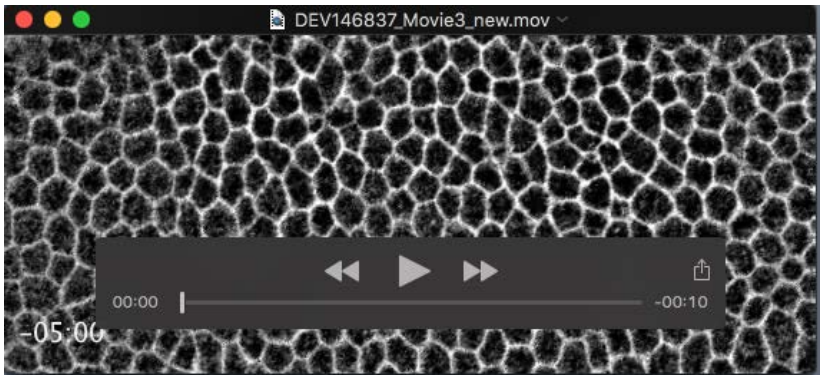

Movie 3. Rosette rearrangements during *Drosophila* axis elongation. Wild-type embryo expressing Spider:GFP. Time indicated in min:s, images acquired every 15 s. Anterior left, ventral down. Rosettes of 5 or more cells are highlighted in random colors.

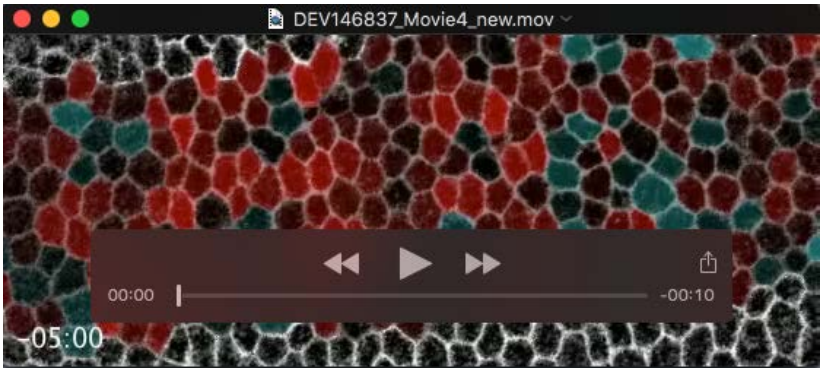

Movie 4. Cell-shape changes during *Drosophila* axis elongation. Wild-type embryo expressing Spider:GFP. Time indicated in min:s, images acquired every 15 s. Anterior left, ventral down. Cells are color-coded based on their width-to-height ratio (smoothed over a seven-frame window). Dorsal-ventral (vertically) elongated cells in red and anterior-posterior (horizontally) elongated cells in blue. More opaque colors indicate a greater degree of elongation.